Int. J. Heat Mass Transfer. Vol. 22, pp. 1407–1415

0017-9310/79/1001-1407 $02.00/0

A MODEL FOR THE EFFECT OF DROPLET INTERACTIONS ON VAPORIZATION

JULIAN M. TISHKOFF
Senior Research Engineer, General Motors Research Laboratories,
Fluid Dynamics Department, General Motors Technical Center,
Warren, MI 48090, U.S.A.

(*Received* 7 *September* 1978 *and in revised form* 2 *November* 1978)

Abstract—Effects of droplet interactions on vaporization were simulated by evaporation of a droplet inside a "bubble". Initially the droplet-in-bubble vaporization rate exceeded that of a single droplet. Subsequently vaporization was retarded by cooling and vapor addition. If the bubble was not much larger than the droplet, saturation occurred before complete vaporization. With increasing bubble size the droplet radius at saturation was diminished until complete vaporization ensued. This saturation-complete vaporization transition was sensitive to pressure and initial gaseous temperature and insensitive to volatility and vapor content. A correlation was developed to incorporate interactions into spray vaporization models.

NOMENCLATURE

A, constant in the approximation for vapor pressure [K];
α, vaporization rate correlation parameter;
B, constant in the approximation for vapor pressure;
C_p, specific heat at constant pressure [J/kg·K];
C_{liq}, liquid phase specific heat [J/kg·K];
D, binary diffusion coefficient [m^2/s];
F, bubble parameter $r_{S,I}/r_{E,I}$;
k, thermal conductivity [W/m·K];
$\mathscr{L}$, latent heat of vaporization [J/kg];
M, dimensionless vaporization rate, $\dot{m}/(4\pi\mu r_{S,I})$;
m, mass [kg];
$\dot{m}$, vaporization rate [kg/s];
n, vaporization rate correlation parameter;
P, pressure [Pa];
Pr, Prandtl number, $C_p\mu/k$;
$\mathbf{q}$, heat flux vector [W/m^2];
R, dimensionless droplet radius, $r_S/r_{S,I}$;
R^0, universal gas constant [8.32 J/(mol·K)];
r, radial spherical coordinate [m];
S, saturation parameter, $r_{s,sat}/r_{S,I}$;
Sc, Schmidt number, $\mu/(\rho D)$;
T, temperature [K];
T_0, integration constant in the temperature solution [K];
t, time [s];
V, radial diffusion velocity [m/s];
v, radial bulk velocity [m/s];
W, molecular weight [kg/mol];
Y, vapor mass fraction;
β, bubble parameter $r_{E,I}/r_{S,I}$;
ρ, mass density [kg/m^3];
τ, vaporization parameter t_{fo}/t_f.

Subscripts

air, air property;
C, critical condition;
E, value at the bubble surface;
f, complete vaporization;
HC, hydrocarbon property;
I, initial value;
liq, liquid hydrocarbon property;
R, reference value;
S, value at the droplet surface;
sat, saturation condition in the bubble;
v, equilibrium vapor state;
0, single droplet value;
∞, ambient condition far from a single droplet.

INTRODUCTION

THE STEADY-STATE combustion of liquid fuel sprays and spray transport and vaporization prior to ignition for transient combustion processes, such as the operation of reciprocating internal combustion engines, have received considerable attention. Much of the analytical work for both spray combustion [1, 2]* and vaporization [3–8] has described the overall disappearance of the liquid phase in terms of the superposition of individual droplet burning or vaporization without interactions among droplets. Experimental observations [9, 10], however, have suggested that for certain examples of spray combustion in which droplets are closely spaced deviations from single droplet behavior occur. These experimental results have motivated a set of modeling efforts aimed at describing a "group" mode of spray combustion [11–14] and vaporization [15].

*Numbers in brackets denote References which are at the end of the report.

The present work develops a model for the effects of droplet interactions on vaporization based on a "droplet-in-bubble" concept previously used by Zung [16]. The basic premise of the model is that in an array of closely spaced droplets symmetry considerations with respect to adjacent droplets dictate that the gas-phase region with which each droplet can exchange enthalpy and mass be limited to a finite "bubble". A simplified and idealized model employing spherical symmetry will be used and is illustrated in Fig. 1. The droplet radius is r_S, while the surrounding bubble radius is r_E. This model represents a more simplistic treatment of droplet interactions than that of Labowsky [15]. However,

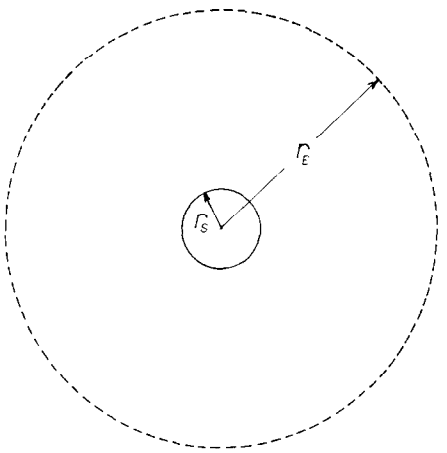

FIG. 1. Droplet-in-bubble vaporization model schematic.

this latter work is restricted to quasi-static spray vaporization without forced convection and is computationally too complex for incorporation within a broader combustion model. The objectives of the present study are: to produce mathematically simple corrections for droplet interaction effects on vaporization which can be added to models for spray vaporization and combustion without large increases in computational requirements; and to study the phenomenon of saturation which has been observed experimentally in spray combustion in regions of closely spaced droplets [10] and can occur also for spray vaporization.

ANALYSIS

Describing equations

The differential equations for the conservation of chemical species and energy in the vaporization process generally must include both unsteady and convective terms. These equations then can be solved only numerically if time variations in the gas-phase transport properties are considered [17].

For the present investigation the following assumptions were adopted:

1. The vaporization process is quasi-steady;
2. The vaporization is spherically symmetric;
3. The total static gas-phase pressure in the bubble is spatially invariant;
4. The conservation equations for chemical species and enthalpy consist of a balance between convection and diffusion;
5. The droplet is composed of a single chemical species, while the gas in the bubble consists of air and vapor from the droplet;
6. Pressures and temperatures are below the critical thermodynamic state of the droplet so that its surface is impermeable to air.

The validity of assumptions 1–4 has been discussed by Williams [18] for the combustion of single droplets. These arguments can be applied to the present model if the flame front is replaced by the bubble surface and chemical reactions do not occur.

The results of both Hubbard, Denny and Mills [17] and Crespo and Liñan [19] indicate that the neglect of unsteadiness in the conservation equations leads to negligible error for the temperature and vapor concentration profiles. Assumption 5 allows the description of mass diffusion by a single equation and simplifies the description of transport properties. The conservation equations for mass, fuel vapor and enthalpy, respectively, are expressed as [17] (the reader should refer to the list of symbols):

$$\frac{1}{r^2}\frac{\mathrm{d}}{\mathrm{d}r}(r^2\rho v) = 0 \tag{1}$$

$$v\frac{\mathrm{d}Y}{\mathrm{d}r} = \frac{1}{\rho r^2}\frac{\mathrm{d}}{\mathrm{d}r}\left(\frac{\mu}{Sc}r^2\frac{\mathrm{d}Y}{\mathrm{d}r}\right) \tag{2}$$

$$v\frac{\mathrm{d}T}{\mathrm{d}r} = \frac{1}{\rho r^2}\frac{\mathrm{d}}{\mathrm{d}r}\left(\frac{\mu}{Pr}r^2\frac{\mathrm{d}T}{\mathrm{d}r}\right). \tag{3}$$

Transport property representation

The integration of equations (2) and (3) requires specification of the variation of the viscosity, μ, and the Schmidt and Prandtl numbers. Also, during vaporization the gaseous portion of the bubble can go from an unsaturated condition to a saturated state, producing large variations in temperature and chemical composition. To account for these effects the transport properties in the two equations were taken to be spatially invariant, but changing with time. The viscosity, μ, thermal conductivity, k, and mass density, ρ, were evaluated at the temperature and vapor mass fraction, T_R and Y_R, respectively, suggested by Hubbard, Denny and Mills [17]:

$$T_R = T_S + (T_E - T_S)/3. \tag{4}$$

$$Y_R = Y_S + (Y_E - Y_S)/3. \tag{5}$$

The binary diffusivity, D, was calculated at T_R. Because the vaporization process was assumed to be quasi-steady and the droplet surface was impermeable to air, the specific heat of the mixture, C_p, becomes that of the hydrocarbon vapor only. A proof of this argument is given in the Appendix. C_p was evaluated at T_R. Expressions for C_p, k, and D were taken from Kent [20]; μ was calculated from

the Lennard–Jones kinetic theory model [21]. ρ was evaluated from the ideal gas law:

$$\rho = \frac{P}{R^0 T\left[\frac{Y}{W} + \frac{(1-Y)}{W_{air}}\right]}. \quad (6)$$

The accuracy of the "1/3" reference property model was tested by comparing estimates for the vaporization of a droplet in an unbounded gaseous volume with those of Kent [20]. The Kent formulation describes droplet vaporization by a quasi-steady model with spatially varying transport properties. An example of this comparison is given in Fig. 2, which shows the wet bulb temperature, T_S, and the vaporization constant, $\dot{m}/r_S$, of a heptane droplet as functions of ambient temperature at a pressure of 506.5 kPa and zero ambient vapor mass fraction.

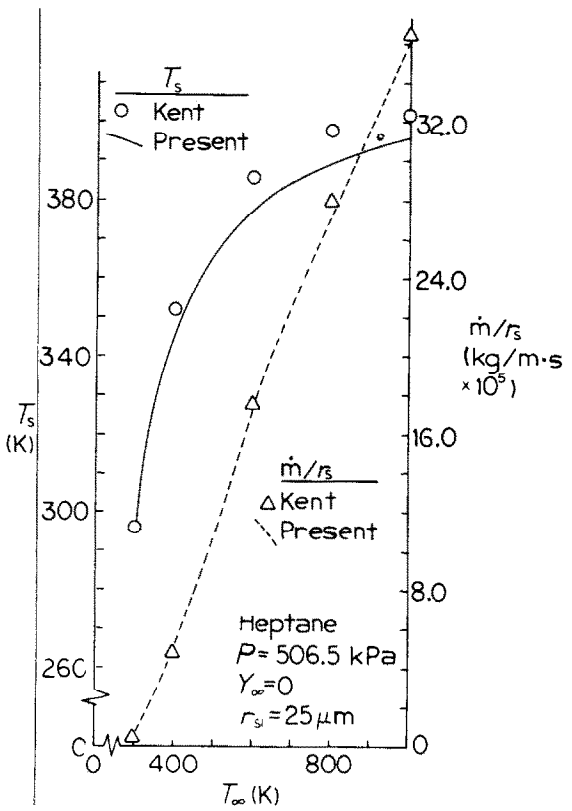

FIG. 2. Single droplet wet bulb temperature, T_s, and vaporization constant, $\dot{m}/r_s$, vs ambient temperature, T_∞.

Agreement within 10 K is obtained between the present results for wet bulb temperature and those of Kent. For the vaporization constant the two results also agree quite well.

Droplet surface boundary conditions

The differential equations given in equations (2)–(3) require four boundary conditions for a unique solution; a fifth relation must be added because of the vaporization rate, $\dot{m} = 4\pi r_S^2 \rho v$, which appears as a parameter in the two differential equations. Two boundary conditions can be expressed from conservation of mass and energy at the droplet surface. The droplet surface was assumed to be impermeable to air. Thus the sum of the mass diffusion and convection there equals the vaporization rate:

$$\dot{m} = 4\pi r_S^2 \rho Y\left[v - \frac{D}{Y}\frac{dY}{dr}\right]. \quad (7)$$

Conservation of energy specifies that heat conducted across the droplet surface supply the latent heat of vaporization and change the droplet temperature, which is uniform [22]:

$$4\pi r_S^2 k \left.\frac{dT}{dr}\right|_{r=r_S} = \dot{m}\mathscr{L} + \tfrac{4}{3}\pi r_S^3 \rho_{liq} C_{liq}\frac{dT_S}{dt}. \quad (8)$$

Bubble surface boundary conditions

The temperature and vapor mass fraction at the bubble surface, T_E and Y_E, respectively, must be specified as functions of time by relations which only can be approximate because the assumption of quasi-steadiness precludes the use of rigorous conservation equations to describe temporal changes. These relations are given in equations (9)–(10):

$$\rho_E C_p \tfrac{4}{3}\pi(r_E^3 - r_S^3)\frac{dT_E}{dt} = -4\pi r_S^2 k \left.\frac{dT}{dr}\right|_{r=r_S} \quad (9)$$

$$\text{and } Y_E = m_{HC}/(m_{HC} + m_{air}), \quad (10)$$

where m_i is the instantaneous mass of the ith species contained in the bubble, and

$$m_{HC} = m_{HC,I} + \int_0^t \dot{m}\,dt'. \quad (11)$$

Calculated results will show that equations (9)–(11) produce physically acceptable results for limiting conditions. As the bubble radius approaches that of the droplet no vaporization occurs, and as the bubble radius grows large vaporization behavior is like that for a single droplet.

Clausius–Clapeyron equation

The final relation required is obtained by assuming that the gas-phase side of the droplet surface is at thermodynamic equilibrium and is saturated with vapor [23]. The vapor pressure, P_v, is given by the Clausius–Clapeyron equation:

$$\frac{dP_v}{dT} = \frac{P_v \mathscr{L}}{R_0 T^2}. \quad (12)$$

Changes in the vapor pressure were calculated from equation (12) with an expression for the latent heat of vaporization, $\mathscr{L}$, developed by Klein [24].

Radial profiles of temperature and vapor mass fraction

Equations (2) and (3) were integrated employing equation (7) and specified values of T_E and Y_E:

$$\frac{Y-1}{Y_E-1} = \exp[MSc(F-1/R)] \quad (13)$$

and

$$\frac{T-T_0}{T_E-T_0}=\exp[MPr(F-1/R)]. \tag{14}$$

Noteworthy in these two equations is the parameter, F, which represents the ratio of the initial values of the droplet and bubble radii. In the limit of single droplet vaporization the value of $F \to 0$, and the solutions assume the familiar form for single droplets.

Vaporization rate calculations

Each droplet-in-bubble vaporization estimate includes three calculations: for the single droplet wet bulb temperature, T_S, and quasi-steady vaporization parameter, M/R; for the initial droplet-in-bubble wet bulb temperature; and for the droplet-in-bubble vaporization history. Initially for the single droplet the vapor pressure at the droplet surface, P_v, is estimated from the approximation of Klein [24] 1 K below the hydrocarbon boiling temperature. The vapor mass fraction, Y_S, then is calculated from

$$\frac{P_v}{P}=\frac{Y_S/W}{Y_S/W+(1-Y_S)/W_{\text{air}}}. \tag{15}$$

The subsequent procedure is common to all three calculations and involves repeated use of the following set of equations in the order given: T_R and Y_R are given by equations (4)–(5); Pr, Sc and μ are computed; the dimensionless vaporization rate, M, comes from equation (13); equation (14) yields the constant T_0; the change in T_S is computed with equation (8); and equation (12) gives the change in P_V.

The two wet bulb temperatures are determined as the value of T_S for which $dT_S/dt = 0$ in equation (8). After each iteration using the steps outlined above the value of dT_S/dt is tested. If the magnitude is unacceptably large, T_S is increased or decreased depending if dT_S/dt is positive or negative, respectively. The single droplet wet bulb temperature is calculated with $F = 0$ in equations (13)–(14).

For the vaporization history calculation the set of steps employed in the wet bulb temperature calculations again is used iteratively, starting at the droplet-in-bubble wet bulb temperature. The set is supplemented by the definitions of M and R to estimate droplet size changes with time and by equations (9)–(11) for the changes in T_E and Y_E. Saturation occurs in the bubble if both $T_S \geqslant T_E$ and $Y_S \leqslant Y_E$. The iteration is halted if saturation is reached or if the droplet is vaporized completely.

First order Taylor series expansions were used to approximate time derivatives, and twelve significant figures were retained for parameters used in these calculations.

RESULTS

Comparison with single droplet theory

The results of this study compare droplet-in-bubble behavior with single droplet vaporization. Relative to a droplet in a bubble the term, "single droplet", refers to a droplet of the same chemical composition and initial temperature in an infinite gaseous medium at the same pressure. The temperature and vapor mass fraction "far" from the surface of the single droplet are the same as the initial values of the corresponding quantities at the bubble surface.

A characterization of results in dimensionless form is given in Fig. 3. A saturation parameter, S, and a vaporization parameter, τ, are plotted semi-logarithmically as functions of a bubble parameter, β. S is the ratio of the droplet radius when saturation conditions are attained in the bubble to the initial droplet radius value, while τ is the time for complete vaporization of a single droplet divided by the droplet-in-bubble vaporization time. The bubble parameter β is the ratio of the initial values of the bubble and droplet radii.

The curves for S and τ both reach zero at a common value of β, which is termed the *transition point* from saturation to complete vaporization.

Certain behavioral characteristics are noteworthy in Fig. 3. The nondimensionalization used makes the curves independent of the initial droplet radius despite the addition of the bubble radius as a second characteristic length. The transition from saturation to complete vaporization in a time of the same order of magnitude as that of a single droplet occurs with a small increase in β. Thirdly, for $\beta > 10^2$ the value of

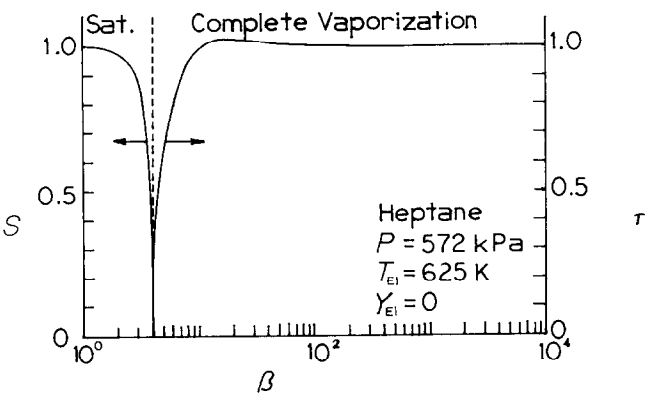

FIG. 3. Saturation parameter, S, and vaporization parameter, τ, vs bubble parameter, β.

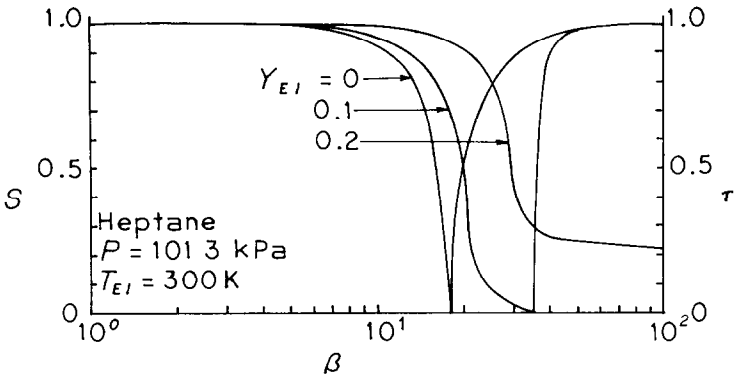

FIG. 4. Saturation parameter, S, and vaporization parameter, τ, vs bubble parameter, β (varying initial vapor mass fraction).

τ approaches unity, indicating that droplet-in-bubble vaporization is the same as that of a single droplet. Therefore, other results which will be reported are restricted to $\beta < 10^2$.

For the range of values $10^1 < \beta < 10^2$ in Fig. 3 τ exceeds unity, indicating that in this regime a droplet in a bubble vaporizes completely in a *shorter* time than that for the corresponding single droplet. The maximum value of this overshoot is small, $\tau = 1.02$ in Fig. 3. An explanation of the overshoot phenomenon can be found from droplet vaporization histories at values of $\beta < 10^2$. The gradients driving the heat and mass-transfer processes controlling vaporization are initially steeper than those for the single droplet because of the finite radius of the bubble. This effect is reflected in the non-zero value of F in equations (13)–(14). Subsequently the addition of the vapor and cooling of the bubble reduce these gradients, slowing the vaporization rate. For $\beta < 10^1$ the gradient reduction effect dominates the vaporization history. However, for $10^1 < \beta < 10^2$ the gradient steepening exerts a slightly stronger influence.

Assumptions about bubble behavior during vaporization

The droplet-in-bubble vaporization model allows the independent variation with time of at most two of the following three bubble parameters: static pressure, total mass and radius. Table 1 summarizes three assumptions investigated in the present study. Calculations produced identical results, shown in Fig. 3, with the elastic, impermeable and rigid, impermeable bubble models and insignificant deviations from this figure with the rigid, permeable bubble model. These calculations lead to the conclusion that deviations from single droplet vaporization behavior result primarily from the finite volume of the bubble relative to the droplet, which is a measure of the capacity of the bubble to support the vaporization process. The remaining calculations to be discussed in this study were made with the elastic, impermeable bubble model.

Parameter sensitivity study

Four parameters can affect the behavior of S and τ as functions of β. These parameters include pressure, fuel volatility, and initial values of the gas-phase temperature and vapor mass fraction. The volatility and vapor mass fraction effects were studied at a pressure of 572 kPa and an initial temperature of 625 K, which represent a relatively high, but subcritical, pressure–temperature condition, of interest in relation to automotive fuel injection.

1. *Fuel volatility.* A decrease in fuel volatility for eight paraffin hydrocarbons extending from propane to dodecane causes only minor deviations from the results of Fig. 3.

2. *Initial vapor mass fraction.* For initial gas-phase conditions in the bubble which do not approach the saturation state of the fuel vapor, the droplet-in-bubble vaporization behavior illustrated in Fig. 3 is

Table 1. Assumed bubble behavior

Bubble description	Constant	Variable	Proposed application
Elastic, impermeable	Mass, pressure	Radius	Spray plume spread in an unbounded environment
Rigid, impermeable	Mass, radius	Pressure	Array of droplets in an enclosure
Rigid, permeable	Pressure, radius	Mass	—

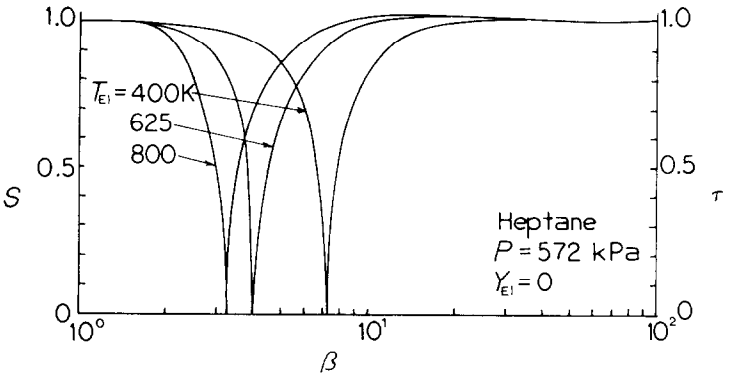

FIG. 5. Saturation parameter, S, and vaporization parameter, τ, vs bubble parameter, β (varying T_{EI} at 572 kPa pressure).

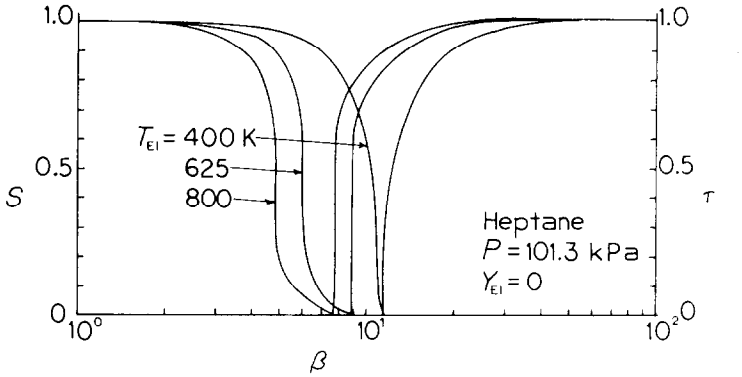

FIG. 6. Saturation parameter, S, and vaporization parameter, τ, vs bubble parameter, β (varying T_{EI} at 101.3 kPa pressure).

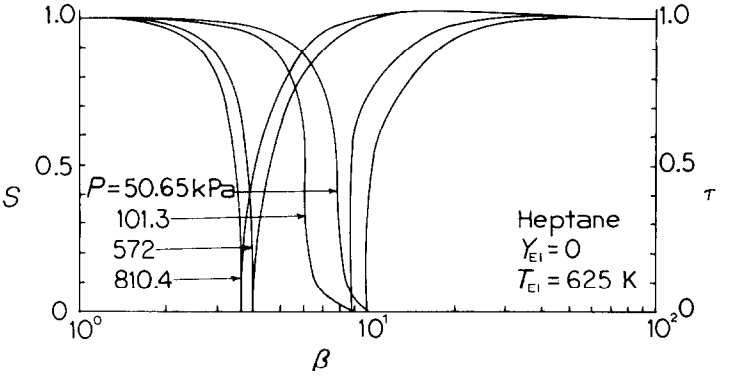

FIG. 7. Saturation parameter, S, and vaporization parameter, τ, vs bubble parameter, β (varying pressure).

insensitive to changes in the initial vapor mass fraction, Y_{EI}. Figure 4 illustrates a deviation from this insensitivity if the initial conditions are close to saturation. Note that the curve for S at $Y_{EI} = 0.2$ in Fig. 4 does not reach zero, so that the droplet does not vaporize completely in the range of bubble sizes corresponding to $1 < \beta \leqslant 100$. Further calculations showed that complete vaporization did not occur for $\beta < 10^4$.

3. *Initial gas-phase temperature, T_{EI}.* Figures 5 and 6 show curves of S and τ vs β for the vaporization of a heptane droplet at zero initial vapor mass fraction and at 572 kPa and 101.3 kPa (atmospheric) pressure, respectively. In each figure curves are plotted at three initial gas-phase temperatures: 400, 625 and 800 K. These figures indicate that the transition point exhibits a strong dependence on T_{EI}, moving to a smaller value of β as T_{EI} is increased. The trend of decreasing S with increasing T_{EI} at fixed β occurs because the saturation vapor pressure in the bubble increases as the temperature is increased.

4. *Gas-phase pressure, P.* The sensitivity of S and τ to P is illustrated in Fig. 7, which gives the variation of S and τ with β for a heptane droplet at 625 K

initial temperature, zero initial vapor mass fraction and four values of P: 50.65, 101.3, 572 and 810.4 kPa. As the pressure is increased the transition moves to a smaller β value. The decrease in S with increasing P at fixed β results from the pressure dependence of the binary diffusivity, which causes the saturation vapor pressure to increase with increasing pressure.

APPLICATION TO SPRAY MODELING

Recent attempts at modeling fuel spray transport phenomena have suggested the need to account for droplet interactions [25]. Limitations on digital computer capacity dictate that droplet interaction submodels include limited calculation steps. This restriction suggests a simple correlation to modify single droplet vaporization models.

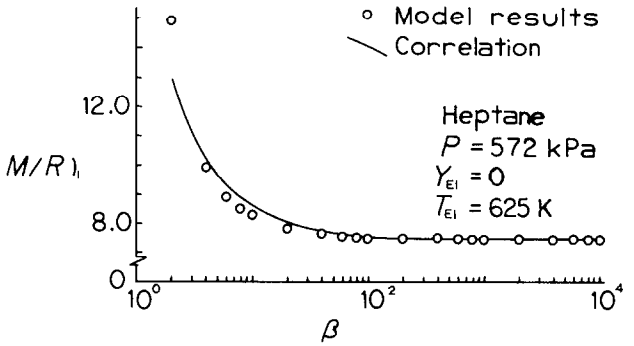

FIG. 8. Initial vaporization parameter, $M/R|_I$, vs bubble parameter, β.

Figure 3 indicates that a correlation based on droplet lifetime behavior would be difficult. Depending on the bubble size relative to the droplet both saturation and complete vaporization must be considered, and the transition between these two circumstances occurs in an essentially discontinuous manner. An alternative correlation which will be presented in this study relates the *initial* droplet-in-bubble vaporization parameter, $M/R|_I$, to the inter-droplet spacing parameter, β. This correlation can be applied to spray vaporization calculations according to the following procedure:

1. At each computation point in the spray calculate single droplet vaporization based on local values of P, T and Y, and evaluate β.
2. Apply the droplet interaction correlation to the single droplet vaporization results.
3. Update the values of T and Y based on vaporization and environmental changes produced by any other coupled models for succeeding calculations.

The form chosen for the correlation is given in equation (16):

$$M/R|_I = \alpha \exp(\beta^n). \tag{16}$$

In expression (16) $M/R|_I$ is given in terms of β through an exponential function including two parameters, α and n. The parameters were evaluated by applying equation (16) to droplet-in-bubble model results with a logarithmic least squares technique [26]. The best-fit results for each test was

$$M/R|_I = M/R|_0 \exp(\beta^{-0.84}), \tag{17}$$

where $M/R|_0$ is the quasi-steady single droplet vaporization parameter. An example of this fit is given in Fig. 8, which show $M/R|_I$ as a function of β. Data points are droplet-in-bubble model results associated with Fig. 3, while the curve is the approximation to the data generated with equation (17).

The application of equation (16) to all droplet-in-bubble computations made in this study indicates that the result of equation (17) is valid at all fuel types, pressures and initial values of temperature and vapor mass fraction tested.

MODEL APPLICATIONS IN ADDITION TO SPRAYS

The results of equations (13), (14) and (17) can be considered to predict the quasi-steady vaporization rate of an isolated single droplet in a turbulent flow field [27]. The numerator of the parameter β can represent the appropriate turbulence transport microscale. Equation (17) might also be applied to modify models of single droplet burning in which the mass transfer from the droplet is calculated on the basis of infinite separation between the droplet surface and the flame front [18].

CLOSING COMMENTS

A droplet-in-bubble model for the vaporization of a single-component fuel droplet into a gaseous medium of finite extent has been developed. This model was used to study the effects of droplet interactions on vaporization within a spray.

The finite gas-phase geometry causes the droplet to vaporize initially faster than the corresponding single droplet. The cooling of the surrounding gaseous medium and the addition of vapor subsequently retard the vaporization rate. If the dimension of the gas is sufficiently small the vaporization process can cease before the droplet is completely vaporized.

Gas-phase pressure and initial gaseous temperature produce large effects on droplet vaporization in a bubble relative to the behavior of single droplets.

Increases in either of these quantities cause the transition from incomplete to complete vaporization to shift to a smaller bubble-droplet radius ratio. The fuel volatility has little influence on droplet vaporization relative to single droplets at the conditions tested. Also the initial vapor mass fraction in the bubble does not affect the vaporization history markedly unless the initial conditions in the bubble are close to the saturated vapor state.

A correlation, given in equation (17), relates droplet-in-bubble vaporization to that of a single droplet. This correlation was developed to contribute to improved models for fuel spray transport.

Acknowledgement –The author is most grateful for the comments, suggestions, and criticism of this work offered by Professor F. A. Williams.

REFERENCES

1. C. E. Polymeropoulos and S. Das, The effect of droplet size on the burning velocity of kerosene–air sprays, *Combust. Flame* **25**, 247–257 (1975).
2. B. Seth and W. A. Sirignano, Unsteady flame propagation through fuel air spray with transient droplet heating, Presented at the Central States Section of the Combustion Institute Meeting, West Lafayette (1978).
3. D. R. Dickinson and W. R. Marshall, The rates of evaporation of sprays, *A.I.Ch.E. Jl* **14**, 541–552 (1968).
4. G. De Jong, Evaporation theory for clouds of fuel droplets, Presented at the Yale Summer Research Program for College Juniors, New Haven (1973).
5. C. K. Law, A theory for monodisperse spray vaporization in adiabatic and isothermal systems, *Int. J. Heat Mass Transfer* **18**, 1285–1292 (1975).
6. C. K. Westbrook, Three dimensional numerical modeling of liquid fuel sprays, in *Sixteenth Symposium (International) on Combustion*. The Combustion Institute, Pittsburgh (1977).
7. C. K. Law, Adiabatic spray vaporization with droplet temperature transient, *Combust. Sci. Technol.* **15**, 65–74 (1977).
8. L. C. Haselman and C. K. Westbrook, A theoretical model for two-phase injection in stratified charge engines, Paper 780318 presented at the S.A.E. Congress and Exposition, Detroit (1978).
9. J. J. Sangiovani and A. S. Kesten, Effect of droplet interaction on ignition in monodispersed droplet streams, in *Sixteenth Symposium (International) on Combustion*. The Combustion Institute, Pittsburgh (1977).
10. N. A. Chigier and A. J. Yule, Vaporization of droplets in high temperature gas streams, Presented at the Physical Chemistry and Hydrodynamics Levich Birthday Conference, Oxford (1977).
11. M. Labowsky and D. E. Rosner, Conditions for "group" combustion in fuel clouds: I. quasi-steady predictions, Presented at the ACS–DW Petroleum Chemistry Symposium on Evaporation and Combustion of Fuel Droplets, San Francisco (1976).
12. H. H. Chiu and T. M. Liu, Group combustion of liquid droplets, *Combust. Sci. Technol.* **17**, 127–142 (1977).
13. H. H. Chiu, R. K. Ahluwalia and B. Koh, Spray group combustion, Paper 78-75 presented at the AIAA Sixteenth Aerospace Sciences Meeting, Huntsville (1978).
14. M. Labowsky, Calculations of the burning rates of interacting fuel particles, Presented at the Central States Section of the Combustion Institute Meeting, West Lafayette (1978).
15. M. Labowsky, The effects of nearest neighbor interactions on the evaporation rate of cloud particles, *Chem. Engng Sci.* **31**, 803–813 (1976).
16. J. T. Zung, Evaporation rate and lifetimes of clouds and sprays in air – the cellular model, *J. Chem. Phys.* **46**, 2064–2070 (1967).
17. G. L. Hubbard, V. E. Denny and A. F. Mills, Droplet evaporation: effects of transients and variable properties, *Int. J. Heat Mass Transfer* **18**, 1003–1008 (1975).
18. F. A. Williams, *Combustion Theory*, p. 47. Addison-Wesley, Reading (1965).
19. A. Crespo and A. Liñan, Unsteady effects in droplet evaporation and combustion, *Combust. Sci. Technol.* **11**, 9–18 (1975).
20. J. C. Kent, Quasi-steady diffusion-controlled droplet vaporization and condensation, *Appl. Scient. Res.* **A28**, 315–359 (1973).
21. J. O. Hirschfelder, C. F. Curtiss and R. B. Bird, *Molecular Theory of Gases and Liquids*, p. 531, John Wiley, New York (1954).
22. C. K. Law, Unsteady droplet combustion with droplet heating, *Combust. Flame* **26**, 17–22 (1976).
23. F. A. Williams, On the assumptions underlying droplet vaporization and combustion, *J. Chem. Phys.* **33**, 133–144 (1960).
24. V. A. Klein, Latent heats of vaporization, A simplified method for calculating engineering data, *Chem. Engng Prog.* **45**, 675–677 (1949).
25. C. K. Westbrook, Numerical solution of the spray equation, Lawrence Livermore Laboratory UCID-17361 (1976).
26. J. M. Tishkoff and C. K. Law, Application of a class of distribution functions to dropsize data by logarithmic least squares techniques, *J. Engng Pwr* **99**, 684–688 (1977).
27. F. A. Williams, Private communication.

APPENDIX

Proof that the Specific Heat of the Mixture is Represented by that of the Hydrocarbon Only

From Williams [18] the vector forms of the conservation equations for chemical species and enthalpy for a droplet composed of species 1 vaporizing in the presence of $n-1$ other gaseous species are, respectively:

$$\nabla \cdot [\rho Y_i(\mathbf{V}_i + \mathbf{v})] = 0 \tag{A1}$$

and

$$\sum_{i=1}^{n} \rho Y_i(\mathbf{v} + \mathbf{V}_i) \cdot \nabla h_i - \nabla \cdot k \nabla T = 0. \tag{A2}$$

Under the assumption of spherical symmetry equation (A1) is integrated to the result

$$r^2 \rho Y_i(V_i + v) = \text{constant}. \tag{A3}$$

Because the droplet surface, $r = r_s$, is impermeable to all but species 1, then the sum of bulk convection and diffusion for each of the other species at $r = r_s$ must equal zero. From equation (A3)

$$r_s^2 \rho Y_i(V_i + v) = 0, \quad i \neq 1. \tag{A4}$$

The application of equation (A4) to equation (A2) completes the proof, since only the enthalpy, hence specific heat, of species 1 appears in the energy conservation relation.

UN MODELE POUR L'EFFET DES INTERACTIONS DE GOUTTES SUR LA VAPORISATION

Résumé—Les effets des intéractions de gouttes sur la vaporisation sont simulés par l'évaporation d'une goutte dans une "bulle". Initialement le flux de vaporisation d'une goutte dans une bulle dépasse celui d'une goutte unique. La vaporisation est retardée par refroidissement et par addition de vapeur. Si la bulle n'est pas plus grande que la goutte, la saturation se produit avant la vaporisation complète. Avec l'accroissement de la taille de la bulle, le rayon de la goutte à la saturation diminue jusqu'à vaporisation complète. Cette transition saturation-vaporisation complète est sensible à la pression et à la température initiale du gaz et elle est insensible à la volatilité et au contenu de vapeur. Une formule est développée pour inclure des intéractions dans les modèles de vaporisation avec pulvérisation.

EIN MODELL FÜR DEN EINFLUSS DER WECHSELWIRKUNGEN ZWISCHEN TROPFEN AUF DIE VERDUNSTUNG

Zusammenfassung—Der Einfluß der Wechselwirkungen zwischen Tropfen auf die Verdunstung wurde durch die Verdunstung eines Tropfens innerhalb einer "Blase" nachvollzogen. Am Anfang des Versuchs überschritt das Maß der Verdunstung in der Blase desjenige eines einzelnen Tropfens. In der Folge wurde die Verdunstung dadurch verzögert, daß gekült und Wasserdampf hinzugefügt wurde. Falls die Blase nicht viel größer als der Tropfen war, trat vor der vollständigen Verdunstung der Sättigungszustand ein. Mit zunehmender Blasengröße wurde der Radius des Tropfens beim Sättigungszustand immer kleiner, bis sich vollständige Verdunstung des Tropfens ergab. Dieser Übergang zur vollständigen Verdunstung bei Sättigung war eine Funktion des Drucks und der Ausgangstemperatur des Gases und war unabhängig von Verdampfungsfähigkeit und Dampfgehalt. Es wurde ein Zusammenhang entwickelt, der die Wechselwirkung von Tropfen in Modellen der Sprühverdunstung miteinzubeziehen gestattet.

МОДЕЛЬ ДЛЯ ИССЛЕДОВАНИЯ ВЛИЯНИЯ ВЗАИМОДЕЙСТВИЯ КАПЕЛЬ НА ПРОЦЕСС ИСПАРЕНИЯ

Аннотация — Влияние взаимодействия капель на процесс испарения исследовалось на модели «капля в пузырьке». Вначале скорость испарения капли в пузырьке превышала скорость испарения единичной капли. Затем испарение затормаживалось за счёт охлаждения и образования пара. Если размеры пузырька не намного превышали размеры капли, насыщение наступало до момента полного испарения. При увеличении размеров пузырька радиус капли в процессе насыщения уменьшался до тех пор, пока не происходило полное испарение. Переход от состояния насыщения к полному испарению зависит от давления и начальной температуры газа и не зависит от летучести и паросодержания. Выведено соотношение для учёта взаимодействия капель в моделях капельного испарения.